J. Fluid Mech. (2008), *vol.* 600, *pp.* 427–443. © 2008 Cambridge University Press
doi:10.1017/S0022112008000566 Printed in the United Kingdom

Onset of wall-attached convection in a rotating fluid layer in the presence of a vertical magnetic field

J. J. SÁNCHEZ-ÁLVAREZ[1], E. CRESPO DEL ARCO[2] AND F. H. BUSSE[3]

[1]ETSI Aeronáuticos, Universidad Politécnica de Madrid, 28040 Madrid, Spain
[2]UNED, Departamento de Física Fundamental, Apdo. 60.141, 28080 Madrid, Spain
[3]Institute of Physics, University of Bayreuth, D-95440 Bayreuth, Germany

(Received 8 May 2007 and in revised form 9 January 2008)

A horizontal fluid layer heated from below and rotating about a vertical axis in the presence of a vertical magnetic field is considered. From earlier work it is known that the onset of convection in a rotating layer usually occurs in the form of travelling waves attached to the vertical sidewalls of the layer. It is found that this behaviour persists when a vertical magnetic field is applied. When the Elsasser number Λ is kept constant and the sidewall is thermally insulating the critical Rayleigh number R_c increases in proportion to the rotation rate described by the square root of the Taylor number, τ. This asymptotic relationship is found for an electrically highly conducting sidewall as well as for an electrically insulating one. At fixed rotation rate for $Q \gg \tau$, R_c grows in proportion to Q when the sidewall is electrically highly conducting, and in proportion to $Q^{3/4}$ when the sidewall is electrically insulating. Here Q is the Chandrasekhar number which is a measure of the magnetic energy density, and a thermally insulating sidewall has been assumed. Of particular interest is the possibility that the magnetic field counteracts the stabilizing influence of rotation on the onset of sidewall convection in the case of thermally insulating sidewalls. When the sidewall is thermally highly conducting, R_c for the sidewall mode grows in proportion to $\tau^{4/3}$. This asymptotic behaviour is found for both cases of electrical boundary conditions, but it no longer precedes the onset of bulk convection for $\Lambda \gtrsim 1$.

1. Introduction

The effect of rotation about a vertical axis on Rayleigh–Bénard convection in a horizontal fluid layer heated from below has been studied for a long time. Early results have been reviewed in (Chandrasekhar 1961, referred to as CH61 in the following). Besides the onset of convection in the bulk of the fluid there exists a second mode of convection supported by the sidewalls of the layer which originally had been predicted as a steady mode by Buell & Catton (1983). Zhong, Ecke & Steinberg (1991) confirmed experimentally the existence of the sidewall mode and demonstrated that it is a travelling wave phenomenon. The correct theory was later given by Goldstein *et al.* (1993).

The influence of a vertical magnetic field on Rayleigh-Bénard convection has also received considerable attention in the past, mainly because of its astrophysical applications. It has been described in detail in CH61 where the combined effect of

rotation and an applied magnetic field is also addressed. Since both rotation and a vertical magnetic field exert a stabilizing influence on the onset of convection it might have been expected that the two effects enhance each other. Chandrasekhar has demonstrated, however, that an applied homogeneous magnetic field can counteract the stabilizing effect of rotation. One of the goals of the analysis of the present paper is to find out whether this phenomenon also occurs in the case of sidewall convection.

The numerical analysis by Goldstein *et al.* (1993) of the onset of sidewall convection in a cylindrical layer has been extended by Herrmann & Busse (1993, referred to as HB93 in the following) and Kuo & Cross (1993) to the case of a straight sidewall. In these papers the influence of the thermal boundary conditions of the sidewall has been emphasized. The critical Rayleigh number R_c, for instance, increases proportionally to the rotation rate when the sidewall is insulating, while it grows with the 4/3 power of the rotation rate when the sidewall is infinitely conducting.

In the system considered in the present work the fluid is electrically conducting and additional properties of the sidewall enter the analysis. We shall restrict attention to cases when the electrical conductivity is either much larger or much lower than that of the fluid. The top and bottom surfaces are assumed to be stress-free and electrically insulating in all cases. The use of these boundary conditions simplifies the analysis and elucidates the mathematical structure of the problem. It is also justified by the property that for large rotation rates the critical Rayleigh number, precession frequency and azimuthal wavenumber of the wall mode converge for stress-free and for no-slip top and bottom surfaces according to Goldstein *et al.* (1993).

The paper starts with the mathematical formulation of the problem and an outline of the numerical methods in § 2. The method of solution is presented in § 3. Results of the numerical study are presented in separate sections for a thermally insulating sidewall, § 4, and for a thermally well-conducting sidewall, § 5. Additional results for smaller Prandtl numbers are included in § 6. A discussion and concluding remarks are given in § 7.

2. Mathematical and numerical models

We consider a horizontal layer (see figure 1) of height d of an electrically conducting fluid, with constant temperatures, T_1 and T_2 with $T_1 < T_2$, at top and bottom boundaries, respectively. The layer is rotating about a vertical axis with an angular velocity $\boldsymbol{\Omega}$ and is in a homogeneous vertical magnetic field with the flux density B_0. We denote by κ, σ and μ the thermal diffusivity, electrical conductivity and magnetic permeability of the fluid, respectively. Using d, d^2/κ, κ/d, $\Delta T \equiv T_2 - T_1$, and B_0 as scales for length, time, velocity, temperature, and magnetic field strength, respectively, we write the equation of motion, the continuity equation, the heat equation for the deviation θ of the temperature from the static distribution, and the equation of magnetic induction in the form

$$(\nabla^2 - P^{-1}\partial_t)\boldsymbol{u} = P^{-1}(\boldsymbol{u}\cdot\nabla\boldsymbol{u} + \nabla p) + \boldsymbol{\tau}\times\boldsymbol{u} - R\theta\hat{\boldsymbol{k}} - Q\left(\hat{\boldsymbol{k}}\cdot\nabla + \frac{\kappa}{\lambda}\boldsymbol{b}\cdot\nabla\right)\boldsymbol{b} \tag{2.1}$$

$$\nabla\cdot\boldsymbol{u} = 0, \tag{2.2}$$

$$(\partial_t + \boldsymbol{u}\cdot\nabla)\,\theta = \boldsymbol{u}\cdot\hat{\boldsymbol{k}} + \nabla^2\theta, \tag{2.3}$$

$$\frac{\kappa}{\lambda}(\partial_t\boldsymbol{b} + \boldsymbol{u}\cdot\nabla\boldsymbol{b} - \boldsymbol{b}\cdot\nabla\boldsymbol{u}) = \nabla^2\boldsymbol{b} + \hat{\boldsymbol{k}}\cdot\nabla\boldsymbol{u}, \tag{2.4}$$

$$\nabla\cdot\boldsymbol{B} = 0. \tag{2.5}$$

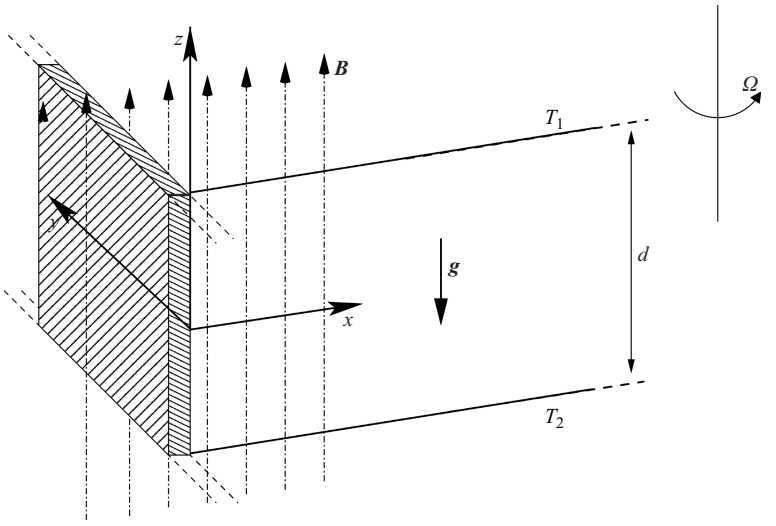

FIGURE 1. Geometrical configuration of the problem of wall-attached convection in the presence of a vertical magnetic field.

Here we have introduced the dimensionless magnetic field in the form $\boldsymbol{B}=\hat{\boldsymbol{k}}+\kappa\boldsymbol{b}/\lambda$, where $\lambda\equiv(\sigma\mu)^{-1}$ is the magnetic diffusivity. The Boussinesq approximation has been assumed and as in previous analytical studies of the onset of sidewall convection in a cylindrical layer (see Goldstein *et al.* 1993; Herrmann & Busse 1993; Kuo & Cross 1993), the centrifugal force has been neglected in comparison to gravity, i.e. $\Omega^2 r_0 \ll g$. This approximation can be satisfied even with $d \ll r_0$ and $\tau \gg 1$ if a sufficiently low kinematic viscosity ν is assumed. For a recent study of the centrifugal effects in rotating convection see Marqués *et al.* (2007).

The problem is characterized by four dimensionless parameters, the Rayleigh, Prandtl, Coriolis and Chandrasekhar numbers, defined, respectively, as

$$R=\alpha g\Delta T d^3/\nu\kappa, \quad P=\nu/\kappa, \quad \tau=2\Omega d^2/\nu, \quad Q=B_0^2 d^2/\rho\mu\nu\lambda. \tag{2.6}$$

In expressions (2.6) α, ν and ρ are the thermal expansion coefficient, kinematic viscosity, and density of the fluid, respectively; g is the gravitational acceleration.

It is convenient to use the following general representation for the solenoidal fields $\boldsymbol{u}$ and $\boldsymbol{b}$:

$$\boldsymbol{u}=\nabla\times(\nabla v\times\hat{\boldsymbol{i}})+\nabla w\times\hat{\boldsymbol{i}}, \tag{2.7}$$

$$\boldsymbol{b}=\nabla\times(\nabla h\times\hat{\boldsymbol{i}})+\nabla\xi\times\hat{\boldsymbol{i}}, \tag{2.8}$$

where v, w and h, ξ describe the poloidal and toroidal components of the velocity and magnetic fields, respectively, and $\hat{\boldsymbol{i}}$ is the unit vector normal to the sidewall and directed into the fluid. In the following a Cartesian system of coordinates will be used with the x-coordinate in the direction of $\hat{\boldsymbol{i}}$ and the z-coordinate in the vertical direction opposite to the direction of gravity. The velocity components are thus given by $(u_x, u_y, u_z)=(-\Delta_2 v, \partial_{xy}v+\partial_z w, \partial_{xz}v-\partial_y w)$ where $\Delta_2\equiv\partial_{yy}^2+\partial_{zz}^2$.

Since liquid metals and some other electrically conducting fluids are characterized by very low values of the ratio κ/λ we shall assume the limit $\kappa/\lambda\ll 1$ and neglect terms of order κ/λ. Applying the operators $\Sigma_1\equiv(0, \partial_z, -\partial_y)$ and $\Sigma_2\equiv(-\Delta_2, \partial_{xy}, \partial_{xz})$

to (2.1), we obtain the following equations for the toroidal and poloidal components of the magnetic and velocity fields, together with rewritten (2.3) for the temperature:

$$(\nabla^2 - P^{-1}\partial_t)\nabla^2\Delta_2 v + R\partial_{xz}\theta - \tau\partial_z\Delta_2 w - Q\partial_{zz}^2\Delta_2 v = 0, \tag{2.9}$$

$$(\nabla^2 - P^{-1}\partial_t)\Delta_2 w + \tau\Delta_2\partial_z v - R\partial_y\theta + Q\partial_z\Delta_2\xi = 0, \tag{2.10}$$

$$\nabla^2\Delta_2\xi + \partial_z\Delta_2 w = 0, \tag{2.11}$$

$$(\nabla^2 - \partial_t)\theta - \partial_y w + \partial_{xz}^2 v = 0. \tag{2.12}$$

Using (2.9)–(2.12) the following equation involving only the toroidal potential of the velocity field can be obtained:

$$\left\{\left[(\nabla^2 - P^{-1}\partial_t)\nabla^2 - Q\partial_{zz}^2\right]^2(\nabla^2 - \partial_t) + \tau^2\nabla^2(\nabla^2 - \partial_t)\partial_{zz}^2 - R\left[(\nabla^2 - P^{-1}\partial_t)\nabla^2 - Q\partial_{zz}^2\right]\left(\partial_{xx}^2 + \partial_{yy}^2\right)\right\}w = 0. \tag{2.13}$$

Since an electrical current, $\boldsymbol{J}$, cannot enter an electrically insulating sidewall, $J_x = 0$ must be required at $x = 0$. At a rigid and electrically well-conducting sidewall $J_y = J_z = 0$ must be required. Accordingly the boundary conditions at the stress-free and electrically insulating top and bottom boundaries and at the rigid sidewall are given by

$$\partial_z v = \partial_{zzz}^3 v = w = \partial_{zz}^2 w = \theta = \partial_z\xi = 0 \text{ at } z = \pm\tfrac{1}{2}. \tag{2.14}$$

$$\left.\begin{array}{l} v = \partial_x v = w = 0 \\ \left.\begin{array}{l}\partial_x\theta\\ \theta\end{array}\right\} = 0 \text{ for thermally } \left\{\begin{array}{ll}\text{insulating} & \text{(I)}\\ \text{conducting} & \text{(C)}\end{array}\right. \\ \left.\begin{array}{l}\partial_x\xi\\ \xi\end{array}\right\} = 0 \text{ for electrically } \left\{\begin{array}{ll}\text{conducting} & \text{(B)}\\ \text{insulating} & \text{(H)}\end{array}\right. \end{array}\right\} \text{ at } x = 0. \tag{2.15}$$

Because of the assumption $\kappa/\lambda \ll 1$ the equation for h

$$\nabla^2\Delta_2 h + \partial_z\Delta_2 v = 0 \tag{2.16}$$

could be directly entered into the Lorentz force term of equation (2.9). Hence h does not enter the analysis and there is no need to specify boundary conditions for it at this point. We shall return to this problem at the end of § 3.

In order to solve the perturbation equations (2.9)–(2.12) we assume that the disturbances are travelling waves in the y-direction, with wavenumber β and frequency ω, and with an exponential decay in the x-direction, perpendicular to the wall. The combination of stress-free boundaries at $z = \pm 1/2$ and a no-slip boundary at $x = 0$ allow separable solutions of the linear problem. The solutions of the constant coefficient equation (2.13) of tenth order in x are given by a linear combination of five exponential functions, decaying in the positive x-direction and characterized by the roots μ_j $(j = 1, \ldots, 5)$. In the axial direction z only the first Fourier mode is considered. We thus propose a solution for the set of equations (2.9)–(2.12) of the form

$$v = \sum_{j=1}^{5} A_j \exp(-\mu_j x + \mathrm{i}\beta y + \mathrm{i}\omega t)\sin(\pi z), \tag{2.17a}$$

$$\theta = \sum_{j=1}^{5} B_j \exp(-\mu_j x + \mathrm{i}\beta y + \mathrm{i}\omega t)\cos(\pi z), \tag{2.17b}$$

$$w = \sum_{j=1}^{5} C_j \exp(-\mu_j x + \mathrm{i}\beta y + \mathrm{i}\omega t)\cos(\pi z), \tag{2.17c}$$

$$\xi = \sum_{j=1}^{5} G_j \exp(-\mu_j x + \mathrm{i}\beta y + \mathrm{i}\omega t)\sin(\pi z), \tag{2.17d}$$

where the constants μ_j are defined as the roots with positive real parts of

$$\hat{q}_j \equiv \mu_j^2 - \beta^2 - \pi^2. \tag{2.18}$$

Here the constants $\hat{q}_j$, $j = 1, \ldots, 5$ are the five roots of

$$\left[\hat{q}\left(\hat{q} - \frac{\mathrm{i}\omega}{P}\right) + Q\pi^2\right]^2 (\hat{q} - \mathrm{i}\omega) - \tau^2\pi^2\hat{q}(\hat{q} - \mathrm{i}\omega) - R\left[\hat{q}\left(\hat{q} - \frac{\mathrm{i}\omega}{P}\right) + Q\pi^2\right](\hat{q} + \pi^2) = 0. \tag{2.19}$$

The coefficients A_j, B_j, C_j, G_j, can be obtained in terms of five unknowns D_j, $j = 1, \ldots, 5$,

$$A_j = D_j\{\beta^2 R\hat{q}_j - (\beta^2 + \pi^2)[\hat{q}_j(\hat{q}_j - \mathrm{i}\omega/P) + Q\pi^2](\hat{q}_j - \mathrm{i}\omega)\}, \tag{2.20a}$$

$$B_j = D_j(\beta^2 + \pi^2)\{\mathrm{i}\beta\hat{q}_j\pi\tau - \mu_j\pi[\hat{q}_j(\hat{q}_j - \mathrm{i}\omega/P) + Q\pi^2]\}, \tag{2.20b}$$

$$C_j = D_j\hat{q}_j[\mathrm{i}\beta\mu_j\pi R + \tau\pi(\beta^2 + \pi^2)(\hat{q}_j - \mathrm{i}\omega)], \tag{2.20c}$$

$$G_j = D_j[\mathrm{i}\beta\mu_j\pi^2 R + \tau\pi^2(\beta^2 + \pi^2)(\hat{q}_j - \mathrm{i}\omega)]. \tag{2.20d}$$

The five unknowns D_j are determined by the boundary conditions (2.15) at $x = 0$,

$$\sum_{j=1}^{5}\{\beta^2 R\hat{q}_j - (\beta^2 + \pi^2)[\hat{q}_j(\hat{q}_j - \mathrm{i}\omega/P) + Q\pi^2](\hat{q}_j - \mathrm{i}\omega)\}D_j = 0, \tag{2.21a}$$

$$\sum_{j=1}^{5}\mu_j\{\beta^2 R\hat{q}_j - (\beta^2 + \pi^2)[\hat{q}_j(\hat{q}_j - \mathrm{i}\omega/P) + Q\pi^2](\hat{q}_j - \mathrm{i}\omega)\}D_j = 0, \tag{2.21b}$$

$$\sum_{j=1}^{5}\hat{f}_j\{\mathrm{i}\beta\hat{q}_j\pi\tau - \mu_j\pi[\hat{q}_j(\hat{q}_j - \mathrm{i}\omega/P) + Q\pi^2]\}D_j = 0, \tag{2.21c}$$

$$\sum_{j=1}^{5}\hat{q}_j[\mathrm{i}\beta\mu_j\pi R + \tau\pi(\beta^2 + \pi^2)(\hat{q}_j - \mathrm{i}\omega)]D_j = 0, \tag{2.21d}$$

$$\sum_{j=1}^{5}\hat{g}_j[\mathrm{i}\beta\mu_j\pi^2 R + \tau\pi^2(\beta^2 + \pi^2)(\hat{q}_j - \mathrm{i}\omega)]D_j = 0. \tag{2.21e}$$

where

$$\hat{f}_j = \begin{Bmatrix}\mu_j\\ 1\end{Bmatrix} \text{ for case } \begin{Bmatrix}\mathrm{I}\\ \mathrm{C}\end{Bmatrix}, \text{ and } \hat{g}_j = \begin{Bmatrix}\mu_j\\ 1\end{Bmatrix} \text{ for case } \begin{Bmatrix}\mathrm{B}\\ \mathrm{H}\end{Bmatrix} \tag{2.22}$$

are used.

3. Method of solution

In order to obtain a solution of the system (2.21) of linear homogeneous equations, the determinant of the coefficient matrix must vanish. It is convenient to rescale the

parameters of the coefficient matrix to reduce their number by one,

$$r \equiv \varepsilon^4 R, \quad \tilde{\omega} \equiv \varepsilon^2 \omega, \quad \check{Q} \equiv \varepsilon^4 Q, \quad \nu_j \equiv \varepsilon \mu_j, \quad q_j \equiv \nu_j^2 - \varepsilon^2(\beta^2 + \pi^2), \quad j = 1, \ldots, 5, \tag{3.1}$$

where ε is defined by $\varepsilon \equiv (\tau\pi)^{-1/3}$. Equation (2.19) thus becomes

$$\left[q\left(q - \frac{\mathrm{i}\tilde{\omega}}{P}\right) + \check{Q}\pi^2\right]^2 (q - \mathrm{i}\tilde{\omega}) - q(q - \mathrm{i}\tilde{\omega}) - r\left[q\left(q - \frac{\mathrm{i}\tilde{\omega}}{P}\right) + \check{Q}\pi^2\right](q + \varepsilon^2\pi^2) = 0, \tag{3.2}$$

and the condition that the determinant of the homogeneous system (2.21) must vanish can be written in a form without ε:

$$D \equiv \begin{vmatrix} f_1\{\mathrm{i}\beta q_1 - \nu_1\pi[q_1(q_1 - \mathrm{i}\tilde{\omega}/P) + \check{Q}\pi^2]\} & \ldots \\ \beta^2 r q_1 - (\beta^2 + \pi^2)[q_1(q_1 - \mathrm{i}\tilde{\omega}/P) + \check{Q}\pi^2](q_1 - \mathrm{i}\tilde{\omega}) & \ldots \\ \nu_1\{\beta^2 r q_1 - (\beta^2 + \pi^2)[q_1(q_1 - \mathrm{i}\tilde{\omega}/P) + \check{Q}\pi^2](q_1 - \mathrm{i}\tilde{\omega})\} & \ldots \\ q_1[\mathrm{i}\beta\nu_1\pi r + (\beta^2 + \pi^2)(q_1 - \mathrm{i}\tilde{\omega})] & \ldots \\ g_1[\mathrm{i}\beta\nu_1\pi^2 r + \pi(\beta^2 + \pi^2)(q_1 - \mathrm{i}\tilde{\omega})] & \ldots \end{vmatrix} = 0. \tag{3.3}$$

The dots indicate the same columns as the first one except that the subscript 1 is replaced by 2, 3, 4 and 5, respectively. f_j and g_j are the rescaled version of $\hat{f}_j$ and $\hat{g}_j$,

$$f_j = \begin{Bmatrix} \nu_j \\ 1 \end{Bmatrix} \text{ for case } \begin{Bmatrix} \mathrm{I} \\ \mathrm{C} \end{Bmatrix}, \text{ and } g_j = \begin{Bmatrix} \nu_j \\ 1 \end{Bmatrix} \text{ for case } \begin{Bmatrix} \mathrm{B} \\ \mathrm{H} \end{Bmatrix}. \tag{3.4}$$

The goal of the numerical solution is to find the critical parameter values R_c, ω_c and β_c as a function of τ and Q. For given values of τ and Q, R_c is the minimum value as a function of β at which the condition (3.3) can be satisfied. This value of the Rayleigh number is of primary interest since the onset of convection occurs at R_c. The corresponding frequency and wavenumber are ω_c and β_c, respectively. The problem posed by (3.2), (3.3) has been solved numerically with a Newton–Raphson method. For a given set of the parameters τ, Q and β and initial values of r and $\tilde{\omega}$ the roots q_j of (3.2) are determined first. Then the values of r and $\tilde{\omega}$ for which the real and imaginary parts of the determinant (3.3) vanish are obtained through the Newton–Raphson iteration. This procedure must be repeated for a sequence of β-values in order to determine the minimum value of r as a function of β. As a result the critical parameters (R_c, ω_c, β_c) for the onset of sidewall convection can be found for given values of τ and Q.

The boundary condition at the sidewall determines the asymptotic behaviour at large τ. In the case $Q = 0$ the asymptotic behaviour was obtained by HB93. To characterize the system, we also use the Elsasser number Λ, defined as the dimensionless ratio between the magnetic energy and the rotation rate, $\Lambda \equiv Q/\tau$. The results obtained for two electrical boundary conditions are presented in two cases: when the sidewall is thermally insulating and when it is perfectly thermally conducting. Most of the computations have been performed with $P = 1$. The cases $P = 0.1$ and $P = 0.025$ will be considered briefly in a separate section.

Once the problem defined above has been solved we may return to equation (2.16) and determine that part of the distortion of the applied magnetic field described by the poloidal function h. A simple solution of equation (2.16) is given by

$$h = \exp(\mathrm{i}\beta y + \mathrm{i}\omega t)\cos(\pi z)\left(\sum_{j=1}^{5} A_j \frac{\exp(-\mu_j x)}{\beta^2 + \pi^2 - \mu_j^2} + A_0 \exp(-x\sqrt{\beta^2 + \pi^2})\right) \tag{3.5}$$

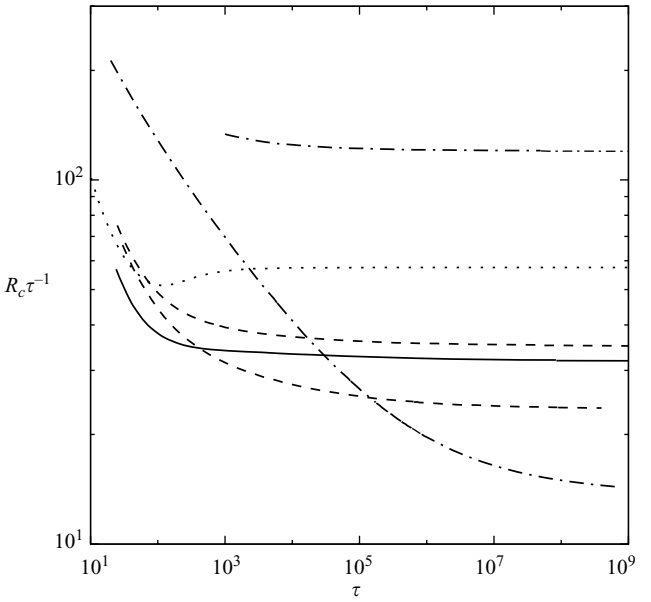

FIGURE 2. The critical Rayleigh number R_c as a function of τ for wall-attached convection with a thermally insulating sidewall and $P = 1$ is obtained numerically for: $Q = 0$ (solid line), $Q = \tau$, electrically insulating sidewall (lower dashed line), $Q = \tau$, electrically conducting sidewall (upper dashed line), $Q = 10\tau$ electrically insulating sidewall (lower dash-dotted line), $Q = 10\tau$ electrically well-conducting sidewall (upper dash-dotted line), and the critical Rayleigh number for bulk convection (CH61) for the case $Q = \tau$ (dotted line).

where A_0 must be chosen such that either $h = 0$ for the electrically highly conducting sidewall or $\partial h/\partial x = h\sqrt{\beta^2 + \pi^2}$ for the insulating sidewall are satisfied at $x = 0$. The latter condition ensures that h and its normal derivative match a potential field in the half-space $x \leqslant 0$. The solution (3.5) corresponds to a periodic continuation of the convection layer in the z-direction which is compatible with the boundary conditions (2.14) and (2.15). But more complex solutions of equation (2.16) could be derived which satisfy other conditions at $z = \pm 0.5$. Because of the rapid decay of the fields v, θ, w, ξ, and h the boundary conditions at $z = \pm 0.5$ are not as important as those at $x = 0$.

4. Results for a thermally insulating sidewall

When there is no magnetic field, $Q = 0$, the asymptotic analysis for large τ (HB93) predicts that the critical Rayleigh number in the case of a thermally insulating sidewall grows proportionally to τ, and that the wavenumber and angular frequency tend to constant values:

$$R_c = \pi^2(6\sqrt{3})^{1/2}\tau, \tag{4.1}$$

$$\beta_c = \pi(2 + \sqrt{3})^{1/2}, \tag{4.2}$$

$$\omega_c = -2\pi\sqrt{3}\beta_c. \tag{4.3}$$

We have obtained the critical conditions at large τ using different values of a fixed Elsasser number. The variation of the critical Rayleigh number with the rotation rate, R_c versus τ, is shown in figure 2 using both limit cases of electrical boundary

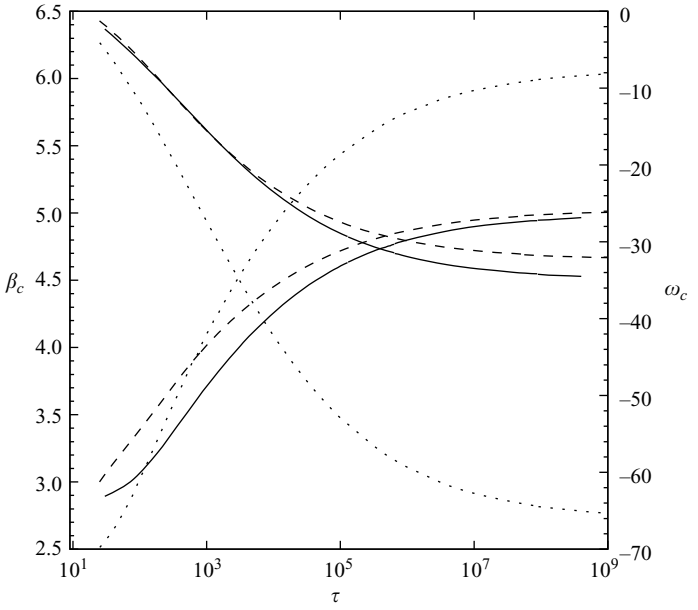

FIGURE 3. The critical wavenumber β_c (ascending lines, left ordinate) and the critical frequency ω_c (descending lines, right ordinate) for wall-attached convection with a thermally insulating sidewall, $P = 1$, and $Q = 0$ (dotted lines), and $Q = \tau$, electrically insulating (solid lines) and electrically highly conducting (dashed lines) sidewall, obtained numerically as function of τ.

conditions, insulating (H) and highly conducting (B), and three different values of the Elsasser number: $\Lambda = 0$, 1, 10. Asymptotically we find $R_c \propto \tau$ which is similar to (4.1). The corresponding critical parameters, β_c and ω_c, are presented in figure 3 for the cases $\Lambda = 1$ and 0. The present results agree with (4.1), (4.2), (4.3) when there is no magnetic field, i.e. $\Lambda = 0$.

The asymptotic behaviour as a function of the Elsasser number is shown in figure 4, where the critical Rayleigh number and the other critical parameters are plotted for both electrical boundary conditions, insulating and highly conducting, at a given value $\tau = 10^8$ of the rotation parameter. For such a value of τ it can be reasonably supposed that the asymptotic limit is reached. It is observed that with an electrically conducting sidewall the magnetic field always stabilizes the static state, even for small values of Λ. When the sidewall is electrically insulating the stabilizing or destabilizing influence of the magnetic field depends on the value of Λ. For $\tau = 10^8$ (see the dotted line in figure 4*a*) an increasing Λ has a destabilizing effect for $\Lambda_m \lesssim 10$ and a stabilizing effect for larger values of Λ.

The property that the magnetic field appears to be more effective in counteracting the stabilizing influence of the Coriolis force at the electrically insulating sidewall than at an electrically well-conducting one, can be traced to the fact that ξ and v both vanish at the insulating sidewall according to condition (2.15). The Lorentz force in equation (2.10) is thus well-correlated with the Coriolis force and can balance the latter more effectively than at a conducting sidewall.

The qualitative behaviour of the critical parameter values as a function of the magnetic field for different values of τ is similar to the behaviour described for $\tau = 10^8$. The variation of the critical Rayleigh number with the Chandrasekhar number, Q, is represented in figure 5 for two values of τ: $\tau = 5 \times 10^3$ and 10^4, and for

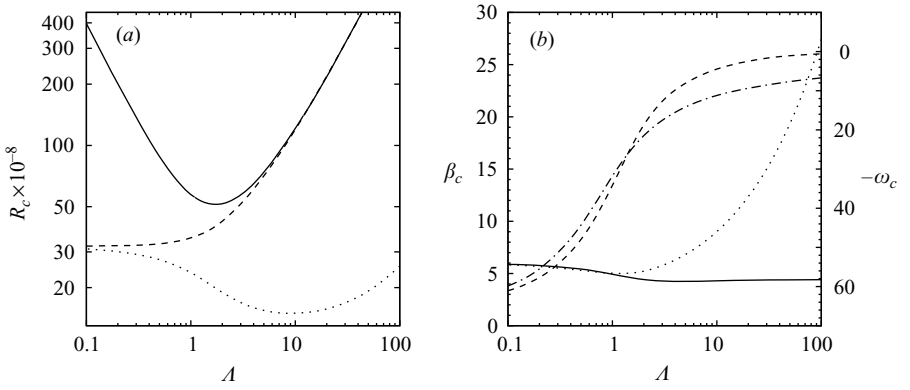

FIGURE 4. (*a*) The critical Rayleigh number R_c as a function of Λ for wall-attached convection with a thermally insulating sidewall, $P=1$ and $\tau=10^8$, obtained for an electrically insulating (dotted line) and an electrically well-conducting (dashed line) sidewall, and the critical Rayleigh number for bulk convection (CH61) at $\tau=10^8$ (solid line). (*b*) The corresponding critical wavenumber β_c (left ordinate) for electrically insulating (solid line) and conducting (dotted line) sidewalls. The critical frequency (right ordinate) ω_c for an electrically insulating (dashed line) and for a highly conducting (dash-dotted line) sidewall is also shown.

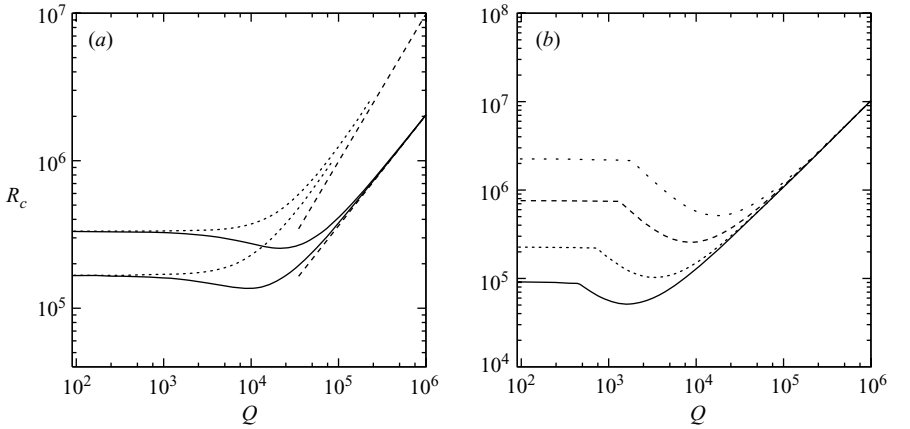

FIGURE 5. (*a*) The critical Rayleigh number R_c as a function of Q for wall-attached convection with $P=1$, and a thermally insulating sidewall. An electrically insulating sidewall (lower solid line for $\tau=5\times10^3$, upper solid line for $\tau=10^4$) yields a minimum of R_c as a function of Q, while an electrically highly conducting sidewall with $\tau=5\times10^3$ (lower dotted line) and with $\tau=10^4$ (upper dotted line) gives rise to monotonic dependence. Dashed lines indicate the functions $R=\pi^2Q$ (upper dashed line) and $R=64.3\,Q^{3/4}$ (lower dashed line). (*b*) The critical Rayleigh number R_c for the onset of bulk convection (CH61), for $\tau=10^3$ (solid line), $\tau=2\times10^3$ (densely dotted line), $\tau=5\times10^3$ (dashed line), $\tau=10^4$ (sparsely dotted line).

both types of electrical conditions at the sidewall, insulating and highly conducting. It is found that when the sidewall is electrically highly conducting the critical Rayleigh number for the wall mode grows with Q at the same rate as the critical Rayleigh number for the onset of convection in the bulk of the layer (CH61): in both cases $R_c\sim\pi^2Q$ is obtained in the limit $Q\gg1$ (see dotted lines in figure 5*a*). When the sidewall is electrically insulating, R_c grows in proportion to $Q^{3/4}$ for $Q\gg1$ (see solid lines in figure 5*a*).

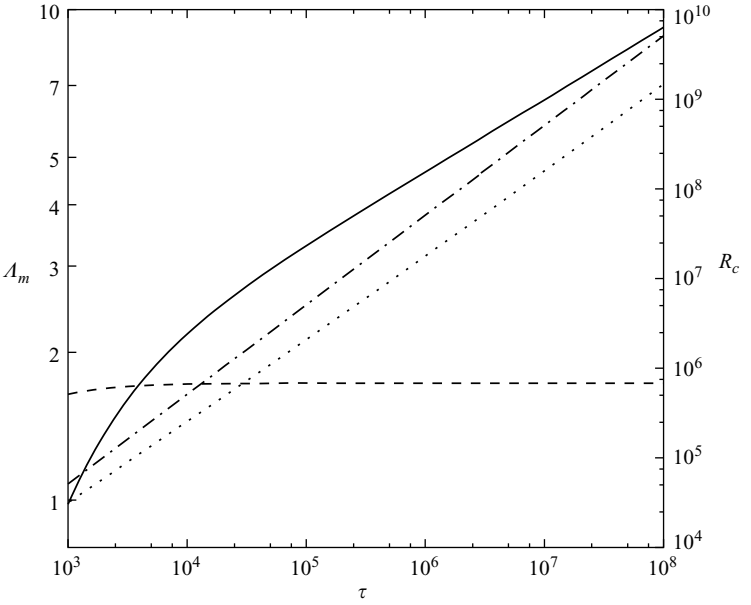

FIGURE 6. The value of $\Lambda_m \equiv Q/\tau$ (left ordinate) where the minimum of the critical Rayleigh number as a function of Q, for a given τ is reached (solid line). The same Λ_m, but for bulk convection is indicated by the dashed line. The corresponding critical values R_c (right ordinate) of Rayleigh number, for wall-attached convection (dotted line) and for bulk convection (CH61) (dash-dotted line) are also shown. All results are for a thermally and electrically insulating sidewall and $P = 1$.

In the case of electrically insulating sidewalls, and for a fixed rotation rate, there exists a value of Q, $Q = Q_m$, where the curve R_c versus Q has a minimum (see figure 5*a*). For $Q < Q_m$ the increasing magnetic field has a destabilizing effect, while for $Q > Q_m$ it tends to stabilize the static fluid layer. We define $\Lambda_m \equiv Q_m/\tau$ and study the dependence of Λ_m on τ. The variation of Λ_m with τ is presented in figure 6 for a large range of τ, from 10^3 to 10^8, for sidewall convection. The values of Λ_m for bulk convection (CH61) corresponding to the minima in figure 5(*b*) are also shown. For the onset of bulk convection and for large rotation rates the minimum of R_c occurs approximately at $\Lambda_m = 1.73$, independently of the value of τ. But for sidewall convection Λ_m increases with τ and exhibits a power-law relationship $\Lambda_m = 0.606\,\tau^{0.148}$.

The convection fields at onset as described by (2.17) at the minimum R_c for $\tau = 10^3$ are shown in figure 7. As can be seen in figure 8, where the vertical velocity is shown for three different values of τ, the boundary layer thickness is proportional to $\tau^{-1/3}$.

5. Results for a thermally highly conducting sidewall

It has been found by HB93 that the critical Rayleigh number for the onset of convection at a thermally well-conducting sidewall is not as low as that obtained for a thermally insulating sidewall. In fact, it was shown in HB93 that the critical conditions for the onset of convection at thermally highly conducting sidewall are given by

$$R_c = 0.9086(\tau\pi)^{4/3} + 2.124(\tau\pi)^{7/6} + o(\tau), \tag{5.1}$$

$$\beta_c = 1.689(\tau\pi)^{1/6} + o(1), \tag{5.2}$$

$$\omega_c = -8.073(\tau\pi)^{1/3} + o\left(\tau^{1/6}\right). \tag{5.3}$$

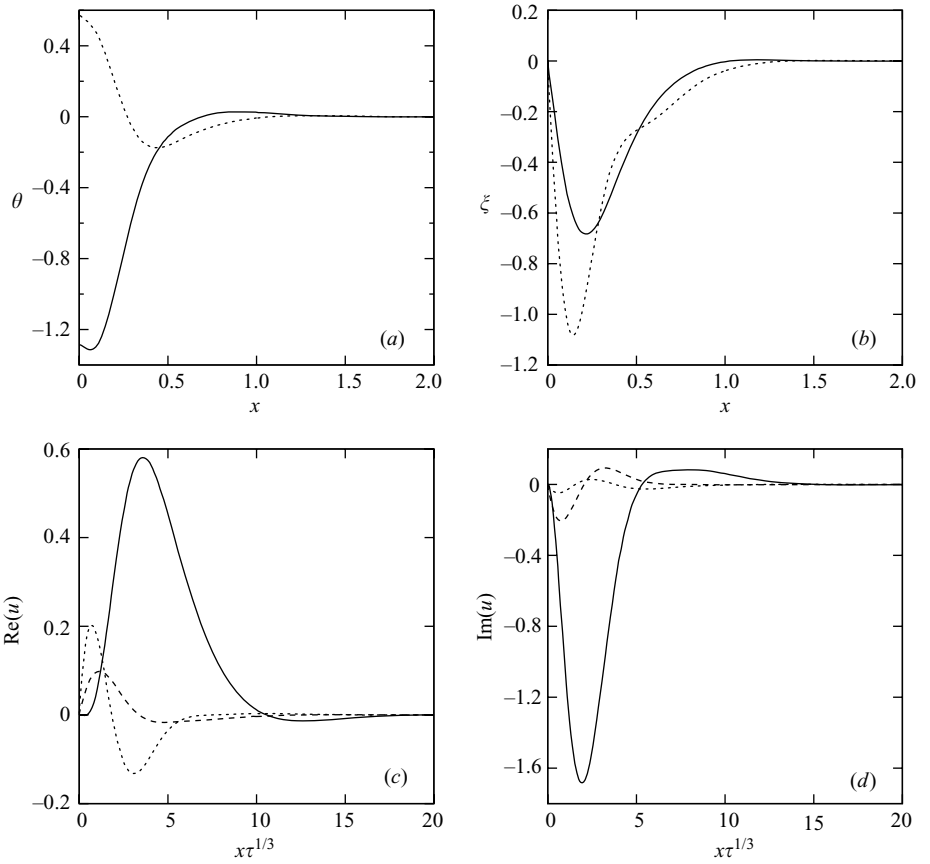

FIGURE 7. Solution as a function of x for $y=0$, $z=-0.25$ for $\tau=10^3$ and $Q=980$ for a thermally and electrically insulating wall. The value of $Q=980$ minimizes the critical value R_c as a function of Q for a fixed $\tau=10^3$. Real (solid line) and imaginary (dashed line) parts of the temperature θ and the toroidal component of the magnetic field ξ are shown in (a) and (b) respectively. Real parts of the velocity $u_x \equiv -\Delta_2 v$ (solid line), $u_y \equiv \tau^{-1/3}(\partial^2_{xy} v + \partial_z w)$ (dotted line), $u_z \equiv \tau^{-1/3}(\partial^2_{xz} v - \partial_y w)$ (dashed line) are shown in (c), while the corresponding imaginary parts of u_x (solid line), u_y (dotted line), u_z (dashed line) are plotted in (d).

The Rayleigh number of wall-attached convection thus exhibits the same power-law dependence on τ as for the onset of bulk convection (CH61). In the presence of a vertical magnetic field this behaviour persists when the Elsasser number is kept constant independently of which electrical boundary condition is chosen. In figure 9 the results obtained for both electrical insulating and highly conducting sidewalls, are shown for a constant value of Elsasser number, $\Lambda=0.1$. It is found that for a given rotation rate the system with an electrically well-conducting sidewall has a higher value of R_c than the system with an insulating one. However when τ is increased the influence of the magnetic field on the value of R_c decreases, and the critical Rayleigh numbers for both cases, electrically insulating and highly conducting, approach the same value, namely the value predicted by HB93 for $Q=0$ (see figure 9a). The frequencies ω_c behave differently, however. The asymptotic value for the electrically insulating wall is larger in absolute value than the value for the highly conducting wall and both values are different from the value in the case $Q=0$. The critical wavenumber β_c is modified by the magnetic field and reaches higher values when the sidewall is electrically highly conducting

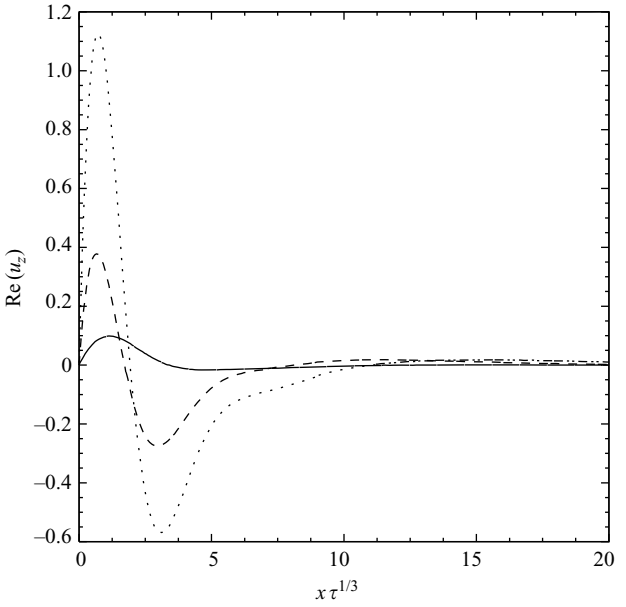

FIGURE 8. Real part of the vertical velocity $u_z \equiv \tau^{-1/3}(\partial_{xz}^2 v - \partial_y w)$ as a function of x for $y = 0$, $z = -0.25$, and for $\tau = 10^3$, $Q = 980$ (solid line), $\tau = 5000$, $Q = 9220$ (dashed line), and $\tau = 10^4$, $Q = 21800$ (dotted line) for a thermally and electrically insulating wall. In each case the value of Q minimizes the critical value R_c as a function of Q for the corresponding fixed value of τ.

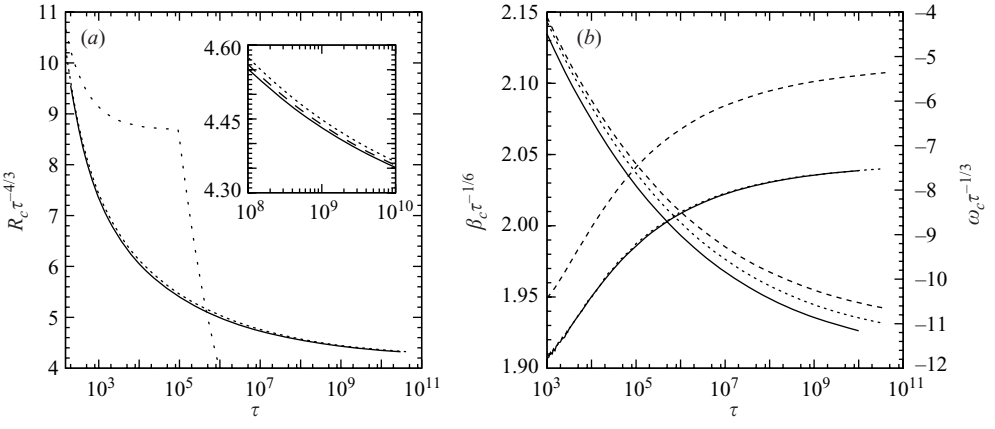

FIGURE 9. (*a*) The critical Rayleigh number R_c as a function of τ for wall-attached convection with a thermally conducting sidewall and $P = 1$, numerically obtained for $Q = 0$ (long dashed line, mainly obscured by the other lines), and $\Lambda = 0.1$ with electrically insulating (solid line) and electrically highly conducting (dotted line) sidewalls. The critical Rayleigh number R_c for the onset of bulk convection (CH61) with $\Lambda = 0.1$ is indicated with the less densely dotted line. (*b*) The critical wavenumber β_c (ascending lines, left ordinate) and the critical frequency ω_c (descending lines, right ordinate) as a function of τ for wall-attached convection with a thermally conducting sidewall and $P = 1$, obtained for $Q = 0$ (solid lines), and $\Lambda = 0.1$ with electrically insulating (dotted lines) and electrically conducting (dashed lines) sidewalls.

than when it is insulating. In the former case, for large τ β_c approaches the same value (5.2) as was predicted in HB93 for $Q = 0$. This behaviour is demonstrated in figure 9(*b*).

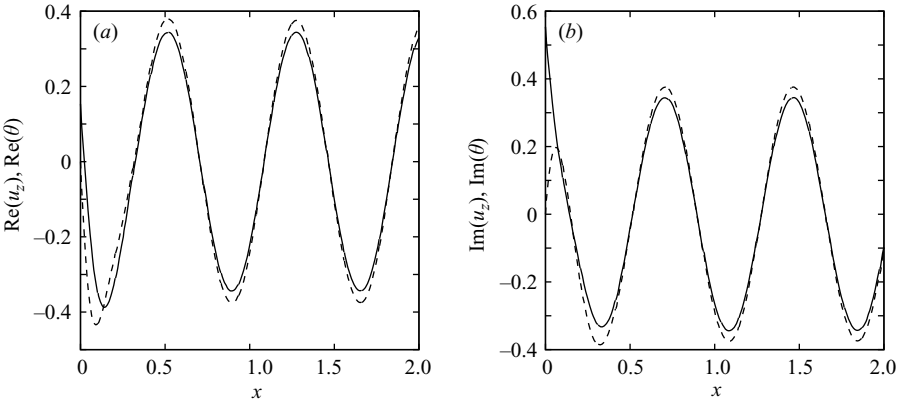

FIGURE 10. Solution as a function of x for $y = 0$, $z = -0.25$ for $\tau = 5000$ and $Q = 9400$. (a) Real part of the vertical velocity $u_z \equiv \tau^{-1/3}(\partial_{xz}^2 v - \partial_y w)$ (solid line) and temperature (dashed line). (b) Imaginary part of the vertical velocity (solid line) and temperature (dashed line).

Convection in the presence of a thermally well-conducting sidewall has in common with convection in the bulk that vertical velocity and temperature go through zero together, in contrast to the thermally insulating sidewall where θ remains finite at the wall while u_z vanishes there. This property of the thermally well-conducting sidewall facilitates a connection between sidewall convection and bulk convection which is apparent in the solution obtained for $\tau = 5000$, $Q = 9400$ as shown in figure 10(a). The merger between sidewall convection and bulk convection requires, of course, that the Rayleigh numbers for both modes coincide. This is the case at the particular point of figure 10(a) in the parameter space, which corresponds to the end of the line for the onset of the sidewall mode for an electrically insulating wall shown in figure 11(a). Here the sidewall mode no longer precedes the onset of bulk convection and merges with a bulk mode in a Takens–Bogdanov bifurcation as is evident from the vanishing of the frequency at that point as shown in figure 11(c). The azimuthal wavenumber β assumes the value 8.83 at the Takens–Bogdanov point. (The bulk mode satisfies the boundary condition at the sidewall and corresponds to a higher wavenumber than the critical one in the bulk. Its critical Rayleigh number is thus higher than the Chandrasekhar value given by the solid line.) The fate of the corresponding mode for the electrically highly conducting sidewall is entirely analogous to that of the mode with an electrically insulating sidewall. The same behaviour as exhibited in figure 11(a) can be found for all sufficiently large values of τ ($\tau \gtrsim 500$). In contrast to the sidewall mode in the case of an thermally insulating sidewall, the sidewall mode in the case of a thermally conducting wall no longer precedes the onset of bulk convection when the strong dip of the critical bulk Rayleigh number occurs around $\Lambda = 1$. The critical Rayleigh numbers for the sidewall modes corresponding to the two different electrical conditions can no longer be distinguished on the large scale of figure 11(b). As in figure 11(a) R_c for the electrical insulating sidewall decreases with increasing Λ, while R_c for the electrically highly conducting wall increases slightly, at least initially, with Λ.

6. Effect of the Prandtl number

The Prandtl number enters the analysis only in connection with the frequency ω. Since the frequency is usually rather small in comparison with the rotation rate, its

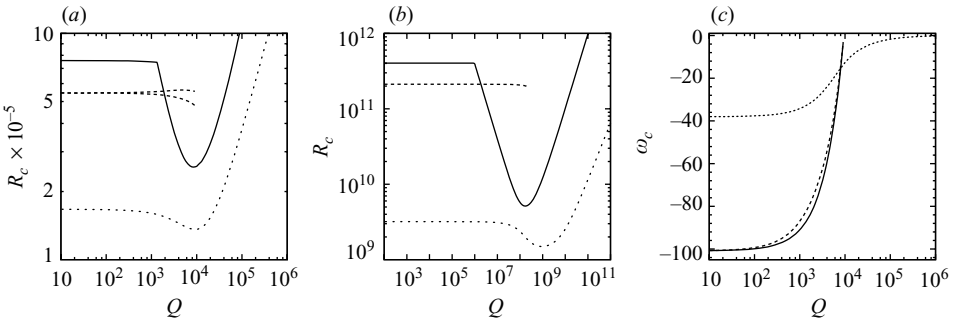

FIGURE 11. The critical Rayleigh number R_c as a function of Q for wall-attached convection with $P = 1$. (*a*) For $\tau = 5000$ and a thermally and electrically insulating wall (dotted line), thermally and electrically conducting wall (upper dashed line), and a thermally conducting and electrically insulating wall (lower dashed line). (*b*) For $\tau = 10^8$ and *a* thermally and electrically insulating wall (dotted line), and a thermally conducting and electrically insulating wall (dashed line). In (*a*) and (*b*) the solid line represents the corresponding critical Rayleigh number for bulk convection (CH61). (*c*) The critical frequency ω_c as a function of Q for wall-attached convection with $P = 1$ for $\tau = 5000$ and a thermally and electrically insulating wall (dotted line), a thermally and electrically conducting wall (dashed line), and a thermally conducting and electrically insulating wall (solid line).

influence on the critical value of the Rayleigh number is quite modest. Only at rather low values of P can a more significant influence on R_c be expected. To study the influence of the Prandtl number we have thus performed computations using several low values of P. For P less than $P_t = 0.67$ the onset of convection is oscillatory in the bulk when the magnetic field strength is low enough (CH61; see values in table 1 for comparisons). The transition Prandtl number P_t usually decreases with increasing strength of the magnetic field. In figure 12(*a*) the effect of P on the critical Rayleigh number for the onset of convection as a function of τ is shown for $\Lambda = 1$ with a thermally and electrically insulating sidewall. Three values of P have been considered: $P = 1$, 0.1, and 0.025. It is found that as in the case of $Q = 0$ (HB93) the onset of wall-attached convection with a thermally insulating sidewall has an asymptotic limit (4.1) that does not depend on the Prandtl number. For $\tau \gg 10^6$, R_c is independent of P, and the critical parameters β_c and ω_c are also independent of P (see figure 12*b*). In figure 12(*c*) the variation of the critical Rayleigh number R_c for the onset of sidewall convection as a function of Q is shown for two different values of the Prandtl number, $P = 1$ and 0.1, with a thermally and electrically insulating sidewall at a fixed $\tau = 5 \times 10^3$. It can be seen that for $Q \leqslant 10^4$ the magnetic field exerts a more destabilizing effect at $P = 0.1$ than at $P = 1$. But for higher values of Q the effect of magnetic field is stabilizing and R_c becomes independent of the Prandtl number. In figure 12(*d*) the values of β_c and ω_c are shown for both cases presented in figure 12(*c*).

7. Concluding remarks

The convection mode attached to a thermally insulating sidewall is the preferred mode of convection at sufficiently high rotation rate. In the case of a thermally well-conducting sidewall it will be preferred, at least for $P \geqslant 0.37$ (HB93). When a magnetic field is applied to the layer, the wall-attached mode continues to be the preferred instability. The electrical boundary condition at the sidewall is a new influence that may determine the stabilizing or destabilizing effect of the magnetic

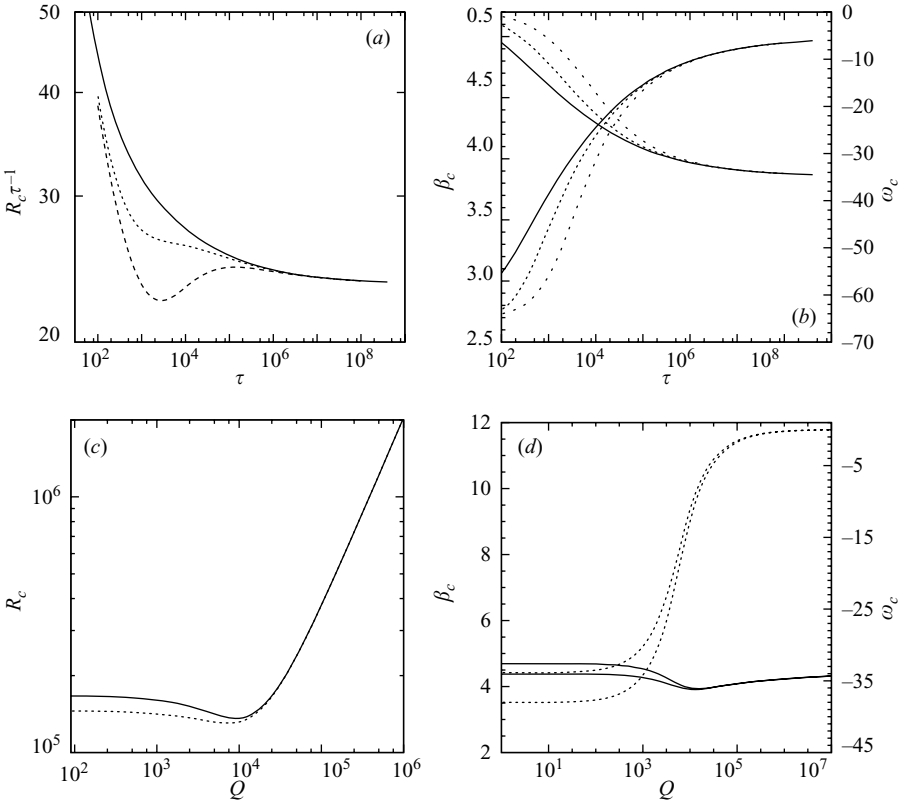

FIGURE 12. (*a*) The critical Rayleigh number R_c for wall-attached convection with a thermally and electrically insulating sidewall as a function of τ, numerically obtained for $Q=\tau$ and $P=1$ (solid line), $P=0.1$ (dotted line), $P=0.025$ (dashed line). (*b*) The corresponding critical wavenumber β_c (ascending lines, left ordinate) and critical frequency ω_c (descending lines, right ordinate) for $P=1$ (solid line), $P=0.1$ (more densely dotted line), $P=0.025$ (dotted line). (*c*) The critical Rayleigh number R_c as a function of Q for wall-attached convection with a thermally and electrically insulating sidewall and $\tau=5\times10^3$, obtained for $P=1$ (solid line), $P=0.1$ (dotted line). (*d*) The corresponding critical wavenumber β_c (solid lines, left ordinate) and the critical frequency ω_c (dotted lines, right ordinate) for $P=1$ (upper solid and lower dotted lines), and $P=0.1$ (lower solid and upper dotted lines).

field on the system. Usually the highly electrically conducting sidewall has a less destabilizing influence on the static state than the insulating wall. This property results from the stronger correlation between Coriolis force and Lorentz force in equation (2.10) caused by the similar x-dependence of v and ξ near the electrically insulating wall such that the magnetic field more effectively counteracts the stabilizing influence of rotation.

When the Elsasser number, $\Lambda=Q/\tau$, is kept constant the critical parameters, R_c, β_c and ω_c, of the wall-attached convection exhibit a dependence on τ that is qualitatively comparable to the case without a magnetic field. At fixed rotation rate the dependence of the critical parameters R_c, β_c on the parameter Q differs from that of the stationary bulk convection described in CH61. In bulk convection the curve $R(\beta)$ has two minima corresponding to cells of different wavenumber for sufficiently high values of Q and τ. The values of these minima near the point where the high-wavenumber minimum is replaced by the low wavenumber minimum in defining the critical value

Q	1300			1500		
Instability	R	β	ω/Ω	R	β	ω/Ω
Bulk stationary I	745444	21.59	–	743312	21.49	–
Bulk stationary II	761588	3.30	–	669953	3.30	–
Bulk oscillatory	134997	11.59	0.1370	143119	11.72	0.1342
Wallmode (IH)	140578	4.25	−0.0583	139873	4.23	−0.0569
Wallmode (IB)	152489	4.33	−0.0573	153620	4.32	−0.0559
Q	5000			5500		
Instability	R	β	ω/Ω	R	β	ω/Ω
Bulk stationary I	–	–	–	–	–	–
Bulk stationary II	286257	3.77	–	276334	3.86	–
Bulk oscillatory	274958	13.17	0.0618	293196	13.32	0.0410
Wallmode (IH)	131690	4.00	−0.0372	131152	3.99	−0.0351
Wallmode (IB)	177706	4.37	−0.0381	181757	4.40	−0.0365

TABLE 1. Critical parameters of wall-attached, bulk stationary and bulk oscillatory convection for $\tau = 5000$ and $P = 0.1$. The instabilities Bulk stationary I and Bulk stationary II correspond to the minima of R as a function of β with high and low wavenumber, respectively.

of the Rayleigh number are shown in the table 1 for $\tau = 5 \times 10^3$ and $P = 0.1$. Such a discontinuity of the critical wavenumber has not been observed in the present case of wall modes. Nevertheless the phenomenon of a non-monotonic dependence of $R_c(Q)$ at given τ can be observed when the sidewall is thermally and electrically insulating.

The influence of the electrical boundary conditions on the onset of convection is much smaller in the case of a thermally well-conducting sidewall than in the case of a thermally insulating sidewall. In contrast to the latter boundary condition the sidewall mode for a thermally well-conducting wall can no longer precede the onset of bulk convection when Λ exceeds a value of order unity and τ is larger than about 500. This property results from the stronger correlation between the Coriolis force and Lorentz force in equation (2.10) caused by the similar x-dependence of v and ξ at the electrically insulating boundary such that the magnetic field more effectively counteracts the stabilizing influence of rotation.

It is worth noting that wall-attached convection and convection in the bulk can coexist quite well. In an analysis of finite-amplitude convection (Bodenschatz, Pesch & Ahlers 2000; Sánchez-Álvarez *et al.* 2005) both patterns have been found for values of the Rayleigh number greater than both of their critical values. In experiments on finite-amplitude convection with vertical magnetic field and vertical axis of rotation we thus expect that steady convection in the bulk can be observed together with travelling sidewall-attached convection. In the case of a thermally insulating sidewall such observations should be possible for all values of the Elsasser number Λ, while the sidewall mode will disappear for $\Lambda \gtrsim 1$ in the case of a thermally well-conducting sidewall.

We gratefully acknowledge Eric Serre and Patrick Bontoux for fruitful discussions. This work has been supported by the Spanish government (research projects No. FIS2004-06596-C02-02 and No. FIS2007-66004-C02-02).

REFERENCES

Bodenschatz, E., Pesch, W. & Ahlers, G. 2000 Recent developments in Rayleigh-Bénard convection. *Annu. Rev. Fluid Mech.* **32**, 709–778.

Buell, J. C. & Catton, I. 1983 Effect of rotation on the stability of a bounded cylindrical layer of fluid heated from below. *Phys. Fluids* **26**, 892–896.

Chandrasekhar, S. 1961 *Hydrodynamic and hydromagnetic stability*. Dover. (Referred to herein as CH61.)

Goldstein, H. F., Knobloch, E., Mercader, I. & Net, M. 1993 Convection in a rotating cylinder. Part 1. Linear theory for moderate Prandtl numbers. *J. Fluid Mech.* **248**, 583–604.

Herrmann, J. & Busse, F. H. 1993 Asymptotic theory of wall-attached convection in a rotating fluid layer. *J. Fluid Mech.* **255**, 183–194. (Referred to herein as HB93.)

Kuo, E. Y. & Cross, M. C. 1993 Traveling-wave wall states in rotating Rayleigh-Bénard convection. *Phys. Rev.* E **47**, R2245–R2248.

Marqués, F., Mercader, I., Batiste, O. & Lopez, J. M. 2007 Centrifugal effects in rotating convection: axisymmetric states and three-dimensional instabilities. *J. Fluid Mech.* **580**, 303–318.

Sánchez-Álvarez, J. J., Serre, E., Crespo del Arco, E. & Busse, F. H. 2005 Square patterns in rotating Rayleigh-Bénard convection. *Phys. Rev.* E **72**, 036307.

Zhong, F., Ecke, R. E. & Steinberg, V. 1991 Asymmetric modes and the transition to vortex structures in rotating Rayleigh-Bénard convection. *Phys. Rev. Lett.* **67**, 2473–2477.